Chemical Modification of Proton Exchanger Sulfonated Polystyrene with Sulfonated Graphene Oxide for Application as a New Polymer Electrolyte Membrane in Direct Methanol Fuel Cell

Mandanipour, Valiollah*+

Department of applied chemistry, University of Gonabad, Gonabad, I.R. IRAN

ABSTRACT: *A novel composite membrane is prepared by the dispersion of Sulfonated Graphene Oxide (SGO) in sulfonated polystyrene–polyethylene (SPS-PE) for electrolyte in the direct methanol fuel cell. For sulfonated polystyrene used the method that was patented by Makowski et al. Graphene Oxide (GO) is prepared by modified Hummer's method and is further functionalized with SO_3-H. SGO is then incorporated into SPS-PE matrix using the solvent cast method to form the composite membrane. The composite membranes are characterized by FT-IR, TGA, and SEM. Oxidative resistance, water uptake, ionic conductivity, and methanol permeability are measured to evaluate its performance in a direct methanol fuel cell with a cation exchanger membrane. The membranes were confirmed to retain 1–5% water vapor at 80–140 °C in the air due to the hydrophilic of highly SPS and SGO. The ionic conductivity and permeability of the membrane to methanol were found to increase with temperature increasing. The membrane SGO-SPS–PE shows the proton conductivity of 2.74×10^{-2} S/cm at 100 °C without extra humidity supply and is very promising for high temperatures with low humidity. The high proton conductivity is ascribed to the unique composition in which the heterocyclic polymer provides the proton motion by construction diffusion and the highly SGO-SPS copolymer retains water vapor to lower the activation energy for proton conduction.*

KEYWORDS: *Sulfonated graphene oxide-sulfonated polystyrene–polyethylene; Polymer electrolyte membrane; Methanol permeability; Ionic conductivity.*

INTRODUCTION

A fuel cell (FC) is an electrochemical engine that converts the chemical potential energy of a fuel such as H_2 and CH_3OH into electric power and heat energy [1]. In recent decades, Direct Methanol Fuel Cells (DMFCs) have been drawing large attention because of their potential use as mobile power sources for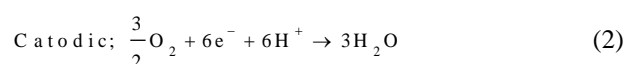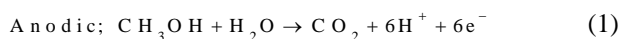 portable electronic devices such as laptops, transportation vehicles, and mobile phones [2-5]. In the DMFCs, polymer electrolyte membranes are the crucial component because separating the anode and cathode, methanol separator between the cathode and anode as well as operate as proton conductors [6-9]. Recently, many researchers the worldwide have conducted research

on the Polymer Electrolyte Membrane Fuel Cells (PEMFC) [10]. Because of the PEMFC are promising green power sources for electronic products [11] with a lot of advantages such as high energy densities, easy operation, and simple fuel supply requirements [12-13].

In a PEMFC, methanol is directly oxidized at the anode in an acidic medium using a proton exchange membrane (PEM). The anodic and cathodic reactions (AR and CR) are as follows [14-15];

$$Anodic; \quad CH_3OH + H_2O \rightarrow CO_2 + 6H^+ + 6e^- \tag{1}$$

$$Catodic; \quad \frac{3}{2}O_2 + 6e^- + 6H^+ \rightarrow 3H_2O \tag{2}$$

In a DMFC, H^+ ions transfer from the anodic side to the cathodic side by passing from a cation exchanger membrane and the overall reaction is;

$$CH_3OH + \frac{3}{2}O_2 \rightarrow CO_2 + 2H_2O \tag{3}$$
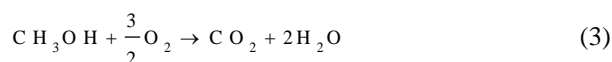
There are two major problems such as the high costs of proton exchange membranes and precious metal catalysts (Pt and Pt/Ru based catalysts) as well as CO poisoning of Pt catalysts at a lower temperature in acidic media have further hampered the development of DMFCs.

The predominant PEMs used in the current DMFCs are Nafion membranes due to their high conductivity, excellent chemical stability, high mechanical properties, flexibility, and long lifetime [16-18]. However, PEMFC based on Nafion technology can generally be operated at below 100 °C with a high humidity supply due to the decrease in the proton conductivity derived from the water evaporation above its boiling point [19]. Indeed, Nafion® has limited application due to low conductivity at temperatures above 80 °C, high cost, and high methanol permeability. Recently, other PEMs with lower methanol permeation was investigated as a possible replacement for Nafion® membrane. Many studies have been focused on developing new materials such as sulfonated poly(styrene divinylbenzene), (SPSD) for PEM. Also, there are done a lot of studies such as poly(5-vinyl tetrazole) and sulfonated polystyrene [19], poly(arylene ether ketone sulfone) [20], poly(arylene ether sulfone) [21], polystyrene-block-poly(ethylene-ran-butylene)-block-polystyrene [22], polybenzimidazoles [23], sulfonated polystyrene/acrylate [24], polyvinylidene fluoride [25],

polyamide with bi-functional sulfonimide bridges [26] and sulfonated polybenzimidazole [27] for development of membranes in PEMs.

Currently, Graphene Oxide (GO) is highly attractive for many applications in supercapacitors, sensors, and fuel cells as a result of its excellent mechanical and thermal properties [28-29]. Graphene Oxide (GO), including a sheet-like graphene framework as an amphiphilic material with hydrophilic regions that contain a carbonyl, hydroxyl, carboxylic, epoxide groups as well as phenol groups on both sides, generally GO is the product of the chemical exfoliation of graphite. [30-31]. GO have a large surface area and electronic insulation property, therefore graphene oxides are particularly attractive as organic fillers in PEMs. The potential advantages of using GOs to improve the performance of DMFCs has not been fully realized, however, GOs could greatly improve the mechanical stability of the PEMs due to their high flexibility and good compatibility with the host materials. Recently studies have illustrated the possibility of using the GOs as fillers in PEMs [32-34]. Currently, we propose here the graphene oxide sheets functionalized by sulfonic acid to produce the Sulfonated Graphene Oxide (SGO) [35]. Graphene oxide sheets are generally sulfonated by various methods including direct oxidation [36], physical adsorption [37], or chemical grafting [38], and then mixed with a polymer to make composite PEMs.

In this study, for the first time, a PEM with a copolymer sulfonated graphene oxide-sulfonated polystyrene-polyethylene (SGO-SPS-PE) as a new PEM was prepared and characterized with different techniques. This PEM 'SGO-SPS-PE' has a hydrophobic PE and SPS backbone and SGO as well as hydrophilic sulfonic acid ($\equiv\!-\!SO_3^-$) ionic groups, which are hydrated by water molecules and transport the H^+ from the anodic side to cathodic side. Several PEM parameters, such as the oxidative resistance, the water uptake, the ionic conductivity, the proton conductivity of the membrane, the methanol permeability of the membrane, and the selectivity of the membrane, were tested.

EXPERIMENTAL SECTION
Materials and apparatuses

All materials and reagents such as methanol, graphite powder, sodium nitrate, sulfuric acid, potassium permanganate, hydrogen peroxide, hydrochloric acid,

dichloromethane and acetic anhydride, 2-propanol, sulfanilic acid, p-Xylene, and polystyrene ($\overline{M} = 33000$ g.mol^{-1}) were purchased from Merck Company, and used without further purification. Linear Low-Density PolyEthylene (LDPE) with a density 0.92 g. cm^3, surface hardness SD48, tensile strength 20 Mpa, linear expansion 20.0×10^{-5} °C, water adsorption 0.01 %, volume resistivity $1.0 \times 10^{16}\Omega$.cm and melting temperature range 120-160 °C was purchased from Bandar Imam Petrochemistry.

The Fourier Transform InfraRed (FT-IR) spectra of the materials and membranes were taken using a JASCO-460 FT-IR spectrometer. The spectral range was 400-4000 cm^{-1}. The surface morphology and the status of the sample were observed with scanning electron microscopy (SEM) and Energy Dispersive X-ray (EDX) analysis, which was equipped with an SEM instrument (CamScan MV 2300). Dry membranes were manually fractured after cooling in liquid nitrogen. Specimens were sputter-coated with gold (15 nm thickness) and imaged on scanning electron microscopy at 5kV. Thermogravimetric analysis was carried out by a TGA/DSC 1 (TGA Q50) at a heating rate of 10 K/min under a N$_2$ atmosphere at a flow rate of approximately 50 mL/min. The proton conductivity of the membrane was measured using a four-probe method by Electrochemical Impedance Spectroscopy (EIS) with a Zahner potentiostat/galvanostat electrochemical workstation model PGSTAT over a frequency range of 4MHz-1Hz with the oscillating voltage of 5 mV.

Preparation of SPS

For sulfonated polystyrene, we used the method patented by *Makowski et al.* [39-40]. Herein, first prepared the acetyl sulfate solution. This solution was prepared by mixing a constant amount of dichloromethane and acetic anhydride under a nitrogen atmosphere. Then the solution was cooled to 0 °C and 98 % sulfuric acid was slowly added. This reaction mixture was stirred at room temperature until a homogeneous and a clear solution was obtained. During the preparation, an excess of acetic anhydride was used to scavenge any trace of water, if present. The acetyl sulfate was freshly prepared prior to each sulfonation reaction.

For sulfonation reaction, 20 g of PS were dissolved in 500 mL of CH$_2$Cl$_2$ in a round-bottomed flask. The flask containing the solution was heated to 40 °C in order to obtain total solubilization of PS and purged with N$_2$ for 40 min.

Then a freshly prepared acetyl sulfate solution was added to the reaction mixture. The produced mixture was maintained at 40 °C under stirring for 2 h. The solution clear yellow was obtained after adding the sulfonating agent. The reaction was terminated by adding an excess of 2-propanol for 30 min and cooling to room temperature. Finally, the sulfonated polystyrene (SPS) was isolated. The reactions related to the production of acetyl sulfate and SPS are shown in Fig. 1A and 1B, respectively.

Preparation of GO and SGO

Graphite oxide was produced from the natural graphite powders using a modified Hummers method [41]. In a typical synthesis, 2 g graphite powder and 1 g sodium nitrate (NaNO$_3$) were combined in a round bottom flask. 46 mL of concentrated sulfuric acid (H$_2$SO$_4$) was added into the round bottom flask while stirring in an ice bath at 0 °C for 20 min. 6 g potassium permanganate (KMnO$_4$) was added very slowly with vigorous stirring while maintaining the temperature below 20 °C because it is a strong oxidizing agent. The flask was removed from the ice bath and stirred at room temperature for 1 h. 92 mL distilled deionized water was then added drop by drop to generate a significant amount of heat and gas. The mixture was stirred for 1 h. After a further 280 mL of deionized water and 40 mL of hydrogen peroxide (H$_2$O$_2$) 30% were added to neutralize the remaining permanganate. The product was then centrifuged (5000 rpm, 20 min) and washed with an abundant amount of 5% hydrochloric acid (HCl) and deionized water (1:3), then the precipitate was gathered and dried at 70 °C under vacuum for 24 h.

To sulfonate the grapheme oxide, 50 mg graphene oxide was added to 8 mL 0.06 M sulfanilic acid solution at a temperature of 70 °C. With continuous stirring, 2 mL 6 × 10^{-3} M of sodium nitrite solution was added dropwise to the mixture and let stand at 70 °C for 12h. Then the washed SGO solution was dried and SGO powder was obtained for the preparation of SGO-SPS-PE membrane. The reactions related to the production of GO and SGO are shown in Fig. 2.

Preparation of SGO-SPS-PE membrane

At first, 1 g of LDPE was dissolved in 30 mL p-Xylene and stirred at 300 rpm for 2.0 h and 100 °C to form a homogeneous solution, and then 1 g of SPS with 0.1 g of SGO, and were mixed and dissolved in p-Xylene to give a black polymer solution. The solutions were cast on glass
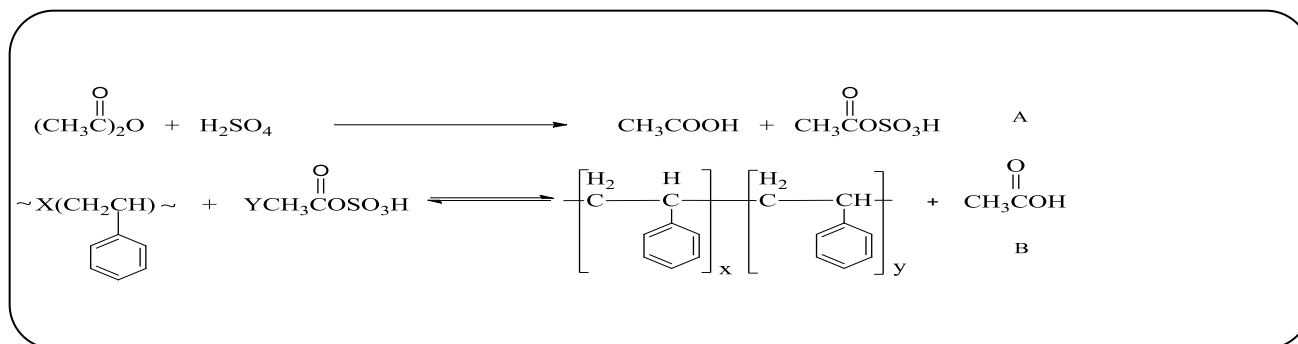
Fig. 1. Reaction scheme of homogeneous sulfonation: (A) acetylsulfate generation and (B) sulfonation of PS.
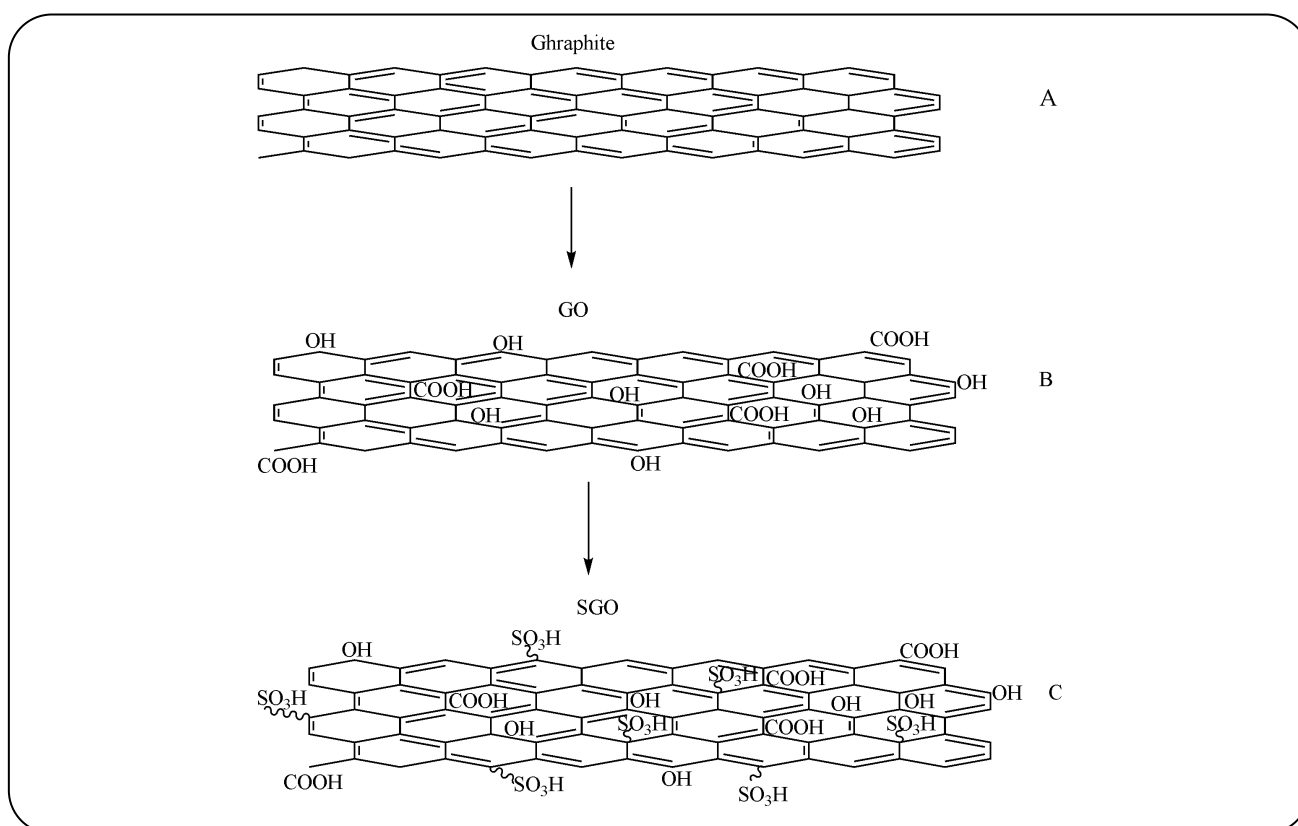

Fig. 2. Schematic representation of sulfonated graphite oxide.

plates and dried at 45 °C for 24 h and then at 75 °C in a vacuum for 12 h. The membrane was peeled off, and designated as SGO-SPS-PE. Before using this PEM "SGO-SPS-PE" in DMAFC, it was converted to the H⁺ form by boiling first in deionized water for 30 min and then in 1 M H_2SO_4 for 24 h. Excess H_2SO_4 was then removed by rinsing and boiling in deionized water. Fig 3. Shown the schematic of SGO-SPS-PE membrane for the direct methanol fuel cell.

Evaluation of membrane properties

To understand the enhanced performance of the proposed membrane as a proton exchange membrane component, different properties such as water uptake rate, ion exchange capacity, methanol permeability, and selectivity factor had major effects and must be measured.

To measure the water retention capability of the membrane, the water uptake was calculated. The water uptake of the composite membrane was determined by measuring
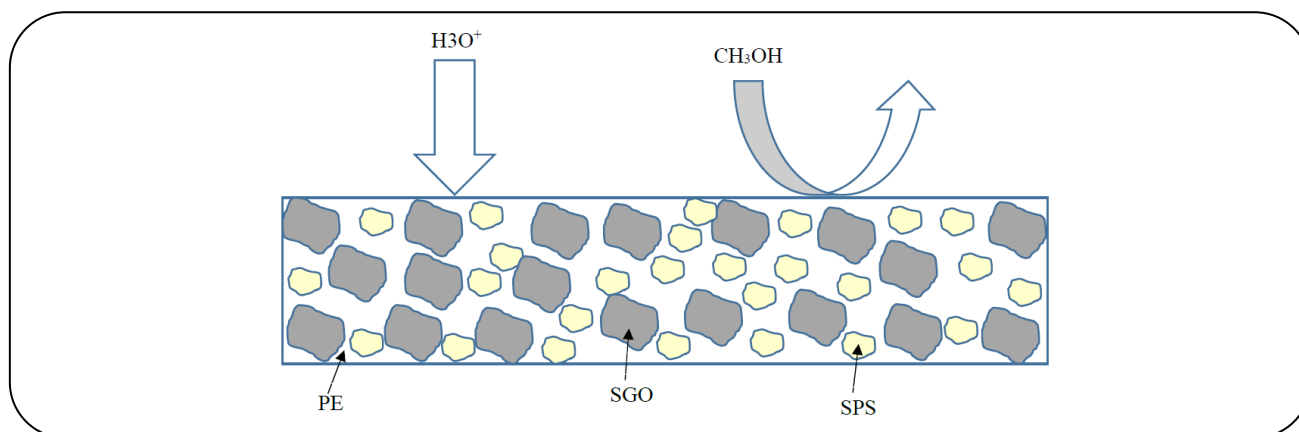
Fig. 3: Schematic of SGO-SPS-PE membrane for the direct methanol fuel cell.

the change in the weight before and after hydration. The membrane was first immersed and saturated in Doubly Distilled Water (DDW) for 24 h. Then, the membrane was weighted quickly after removing the surface water to determine the wetted membrane weight (W_w). The dry membrane weight (W_d) was determined after drying the membrane at 373 K for 2 h. The water uptake was calculated with the following equation [42]:

$$Water\ uptake(\%) = \frac{W_w - W_d}{W_d} \times 100 \tag{4}$$

Ion exchange membrane (IEC) was determined by a back-titration method. At first, the sample was dried until the weight was constant, after which the sample was soaked in 50 mL of a saturated NaCl solution for 24 h to liberate the H^+ ions to the solution by an ion exchange reaction with Na^+ ions. The ion-exchanged solution was titrated with a 0.01 M NaOH solution using phenolphthalein as an indicator. IEC values were calculated by the following equation:

$$IEC = \frac{V_{NaOH} \times C_{NaOH}}{W_{dry}} \tag{5}$$

Where W_{dry} (g) is the dry mass of the membrane, V_{NaOH} (L) is the volume of the titrated NaOH solution and C_{NaOH} (mol/L) is the molar concentration of NaOH in the solution.

Immersing a piece of the membrane into Fenton's reagent under stirring (3% H_2O_2 aqueous solution containing 2 ppm $FeSO_4$) for 1 h at 80 °C was used to investigate membrane durability against free radical species. The oxidative durability was evaluated by recording

the time required to completely dissolve and the maintained weight of the membrane after 2 h in the reagent.

The proton conductivity of the membrane was measured using a four-probe method [42] by Electrochemical Impedance Spectroscopy (EIS) with a Zahner potentiostat/galvanostat electrochemical workstation model PGSTAT over a frequency range of 4MHz-1Hz with the oscillating voltage of 5 mV. For this four-probe method, two inner platinum (Pt) wires (0.2 mm diameter) served as voltage sensors and two outer Pt wires (0.2 mm diameter) served as AC current injectors. The membrane sample, with the size of ca. 3×1.0 cm^2, was sandwiched between two Teflon blocks and held in place with nylon screws. Before the test, the membranes were immersed in a 1.0 M HCl solution for 12 h for activation and then washed with deionized water until pH = 7. The proton conductivity measurements were carried out in the temperature range from 30°C in liquid water. Proton conductivity was calculated from the impedance data according to the following: The proton conductivity (s) was calculated according to the following equation:

$$\sigma = \frac{L}{R\ W\ d} \tag{6}$$

Where σ is the proton conductivity (S/cm), L is the distance between potential-sensing electrodes (cm), R is the membrane resistance R is the resistance associated with the ionic conductivity of a membrane from the impedance data (Ω), W is the width of the membrane (cm) and d is the thickness (cm) of the membrane.

The methanol permeability through the membrane was measured using a custom-built two-compartment diffusion cell.

The membrane was clamped vertically between two glass compartments; each compartment contained a magnetic stirring bar for solution agitation. The feed compartment was filled with 5 M methanol, and the receiving chamber contained deionized water. The methanol concentration of the solution in the receiving compartment was measured. The membrane permeability was calculated with the following equation [42]:

$$P = \frac{1}{C_A}\left(\frac{\Delta C_{B(t)}}{\Delta t}\right)\left(\frac{L\, V_B}{A}\right) \tag{7}$$

Where P is the methanol diffusion permeability of the membrane (cm^2/s), C_A is the concentration of methanol in cell A (mol/L), $\Delta C_{B(t)}/\Delta t$ is the slope of the molar concentration variation of methanol in cell B as a function of time (mol/L.s), V_B is the volume of each diffusion reservoir (cm^3), A is the membrane area (cm^2) and L is the thickness of the membrane (cm).

Finally, the selectivity factor (the ratio of the proton conductivity to the methanol permeability) was determined with the following equation [42]:

$$Selectivity = \frac{\sigma}{P} \tag{8}$$

RESULTS AND DISCUSSION
SEM characterization

SEM provided information about the morphology of the membrane. The SEM measurements were used to characterize the structure of the membrane. Fig. 4a-b show surface micrographs of the SGO (Fig. 4a) and SGO-SPS-PE (Fig. 4b) composite membrane. The SEM image of particles of SGO is shown in Fig. 4a. The image clearly depicts the diameter of particles in the size range of about 100nm-1μm. Fig. 4b shows that the hybrid SGO-SPS-PE uniform matrix membrane had a dense structure. Graphene oxide had been considered an impressive additive in SGO-SPS-PE composite membrane for low methanol permeability and performed excellent DMFC performance. Fig. 4b benefits from the high solubility of the SGO, PE, and the SPS polymers in the para-xylene as a solvent used for the membrane fabrication and the good compatibility between the SPS polymer and the SGO. Therefore, the synthesized film was homogeneous
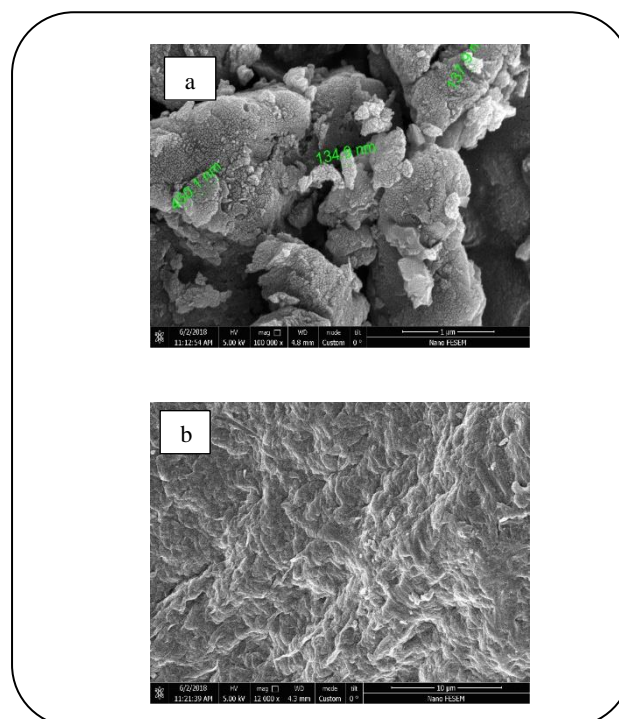

Fig. 4. SEM image for (a) SGO (b) SGO-SPS-PE membrane.

and hence formed a more dense membrane. These graphs illustrate that using SGO promotes the formation of small pores in the PEM.

FT-IR characterization

FT–IR important bands of the PE, SPS, SGO, and SGO-SPS-PE are present in Table 1. The main bands of polyethylene in the IR region are; CH_2 asymmetric strong stretching in 2919 cm^{-1}, CH_2 symmetric strong stretching in 2851 cm^{-1}, bending strong deformation in 1473 and 1463 cm^{-1}, wagging medium deformation in 1366 and 1351 cm^{-1}, twisting weak deformation in 1306 cm^{-1}, wagging very weak deformation in 1176 cm^{-1} and rocking medium deformation in 731–720 cm^{-1}. Table 1 shows the FT-IR important bands of the fresh PS-SO$_3$H powders. The bands at 2925 and 2876 cm^{-1} are due to the aliphatic C-H stretching absorbance of methylene and methylene groups in the main chain. SO_2 asymmetric stretching appears at 1385 cm^{-1}. A strong band at 1652 cm^{-1} indicates an aromatic C=C bond. The four sharp peaks at 1009 cm^{-1}, 1039 cm^{-1}, 1129 cm^{-1}, 1183 cm^{-1} are due to SO_3 symmetric stretching. The bands at around 1619 cm^{-1} are due to deformation and skeletal vibrations of C-H in PS. The bonding of the sulfonic groups to the aromatic ring of crosslinked PS-SO$_3$H is found at 833 cm^{-1} (out of a plane

Table 1: FT-IR important bands for SPS, PE, SGO and SGO-SPS-PE membrane.

Samples	Important Bands (cm^{-1})
SPS	3417, 2925, 2876, 1652, 1619, 1385, 1183, 1129, 1039, 1009, 833
PE	2921, 2851, 1471, 1366, 1351, 1176, 1306, 1083, 731, 719
SGO	3443, 2923, 2892, 1644, 1360, 1240, 1062, 726, 674
SGO-SPS-PE	3416, 2924, 2949, 1617, 1471, 1385, 1179, 1128, 1039, 1009, 833, 776, 718

deformation bands assigned to substituted aromatic ring γ (Car-H)). The strong bands centered at 3432 cm^{-1} can be attributed to the stretching vibration of the acid O-H groups. The strong bands at 2852 cm^{-1} and 2921 cm^{-1} correspond to the C-H stretching vibration of CH_2 groups. The medium bands centered at 1633 cm^{-1} can be attributed to the stretching vibration of the C=C groups of benzenes. The medium bands centered at around 1469 cm^{-1} can be attributed to the bending vibration of the CH_2 groups and C=C aromatic groups. The four sharp bands at 1009 cm^{-1}, 1039 cm^{-1}, 1128 cm^{-1}, 1179 cm^{-1} show clearly SO_3 symmetric stretching as above described. Table 1 shows the FT-IR important bands of the SGO, The strong bands at 1644 cm^{-1} are attributed to the C=O stretching of COOH groups, the bands at 1360 cm^{-1} are attributed to the O–H deformation of C–OH groups, and the bands at 1240 cm^{-1} correspond to the asymmetric stretching of C–O–C groups [43]. The bands at 3443 cm^{-1} for OH group stretching vibration and 1062 cm^{-1} assigned to C-O groups vibration. Table 1 shows the FT-IR important bands of the composite materials prepared by reinforcement of membrane, i.e. adding SGO to SPS-PE**.** The FT-IR studies reveal the formation of composite materials and help to obtain their compositions qualitatively. The strong bands at 2924 cm^{-1} and 2949 cm^{-1} correspond to the C-H stretching vibration of CH_2 groups. The strong bands at 1617 cm^{-1} are attributed to the C=O stretching of COOH groups. The bands at 3416 cm^{-1} for OH group stretching vibration and 1039 cm^{-1} assigned to C-O groups vibration. The bands at 1000-1180 cm^{-1} correspond to the sulfonic acid group in all these compositions, i.e. due to the symmetric –SO_3 stretching as above described. Furthermore, the absorption bands at 1128 cm^{-1} and 1179 cm^{-1} in composite membrane represent the symmetric and asymmetric stretching frequency, respectively, for a sulfonic acid group in SPS that confirms the covalent grafting of SPS on SGO [44]. The characteristic bands of the three components SPS, PE and
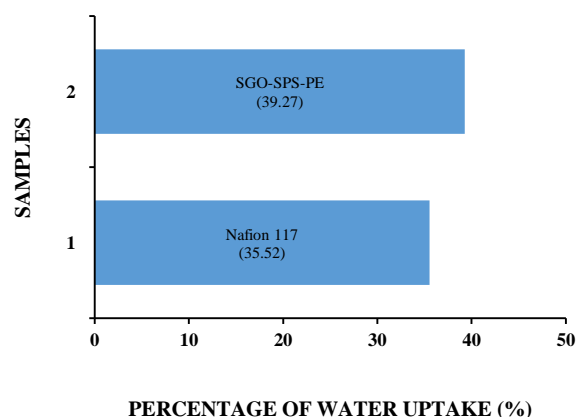
Fig. 5 Water uptake of composite and Nafion® 117 membranes.

SGO confirms the presence of three phases in composite materials, but all these bands show a systematic shifting that indicates the existence of significant interaction between SGO and SPS in the composite materials.

Water uptake

Fig. 5 shows the water content of the Nafion®117 and composite membrane equilibrated with 100% relative humidity air at 25 °C and immersed in liquid water at 25 °C. As shown in Fig. 5, the water content was higher in the composite membrane (39.27%) than in Nafion®117 (35.52%) which is closed to the literature [45]. The water uptake of PEMs is an essential parameter that directly affects proton conductivity and mechanical stability of the membrane and consequently, the overall performance of the DMFC, so a higher water uptake rate may improve the performance of a fuel cell because the water in the membrane can effectively reduce the activation energy of proton transfer by providing more pathways for proton hopping (Grotthus mechanism) and diffusion mechanism (vehicular mechanism) [46]. However, a membrane with excess water content could lead to poor mechanical properties and low stability [47].

Table 2. Ion exchange capacity, proton conductivity, methanol permeability, selectivity, and Oxidative stability factor of the Nafion®117 and composite membrane.

Membrane	IEC (meq.g^{-1})	σ (S.cm)	P (cm^2.s^{-1})	σ / P (S.s.cm^{-3})	Oxidative stability (Wt %)
Nafion®117	0.90	5.30×10^{-2}	29.4×10^{-7}	1.80×10^4	> 97
SGO-SPS-PE	0.96	2.74×10^{-2}	6.12×10^{-7}	4.48×10^4	> 96

Ion exchange capacity, proton conductivity, methanol permeability, selectivity, and oxidative stability

Table 2 summarizes the ion exchange capacity, proton conductivity, methanol permeability, selectivity, and oxidative stability of the Nafion®117 and composite membrane. The IEC is the display of membrane ability for transferring protons from the anodic side to the cathodic side in DMFC. The ion exchange capacity is a good parameter to determine the aggregation of proton exchangeable groups and proton conductivity of membranes. Table 2 shows the result of IEC for Nafion®117 and composite membrane. As shown in Table 2, the composite membrane exhibited a higher IEC value compared to the Nafion®117.

The proton conductivity of the membrane sample was measured at room temperature and 100% relative humidity. We also performed the test composite membrane with water for one day. Table 2 shows the composite membrane had good proton conductivity [48]. The methanol permeability of the membrane sample was measured at room temperature using a 5 M methanol solution. Table 2 shows that methanol permeability in the composite membrane was lower than Nafion®117, therefore, the selectivity factor for the composite membrane was better than Nafion®117. A membrane with low methanol permeability is advantageous for DMFC usage. Because increasing the proton conductivity and decreasing the methanol permeability is the goal with DMFC membranes, the selectivity factor (the ratio of the proton conductivity to the methanol permeability) can be treated as a guide for developing better DMFC membrane characteristics. The higher selectivity factor contributes to better DMFC performance. The selectivity factor results are shown in Table 2.

The results of the oxidation stability investigation of the composite membrane and Nafion®117 were also examined in Fenton's reagent at 80 °C are given in Table 2. As results show, this membrane showed good stability, for which more than 96% of the weight was regained after 1 h. The excellent performance of the membrane in terms of oxidative stability might be due to the formed crosslinking network between the SPS-PE and the SGO.
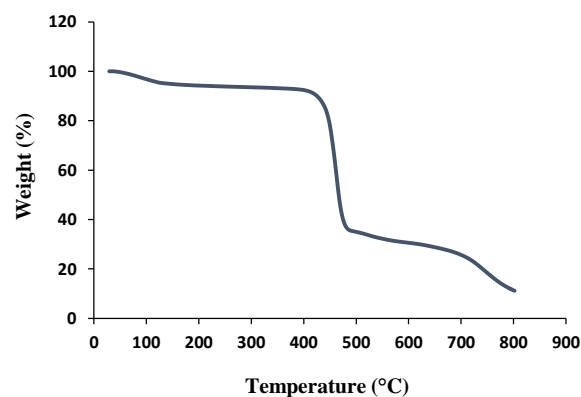

Fig 6: TGA analysis of the SGO-SPS-PE membrane in a temperature range from 30 to 800 °C.

TGA characterizations

Fig. 6 was shown the TGA curves for SGO-SPS-PE. The parameters associated with this weight-loss region exhibit four weight zones degradation. Based on Fig 6, the first weight-loss region is centered around 95–140°C. It is well known that the membrane strongly absorbs water, so this weight loss may be attributed to the loss of absorbed water. The second main weight-loss region is located around 420-480 °C. Weight losses of 47–57% occur in this region. This weight-loss zone seen is associated with the greatest mass loss and is termed, therefore, the main stage. Therefore, this mass loss has been attributed to the complete thermodegradation of the skeletal chain structure of composite. Weight loss occurring above 650 °C for SGO-SPS-PE membrane can be used for the elimination of organic moieties. The weight loss within a range 650–800 °C is due to the decomposition of the polystyrene and SGO [35].

Table 3 was shown a comparison study for degradation temperature of the proposed membrane with some membranes in literature. Based on the results, the degradation temperature of the proposed membrane is higher than other membranes. So, using SGO, the thermal stability increased. Also, the Simultaneous Thermal Analysis (STA) of the proposed membrane was checked

Table 3: Degradation temperature of different membranes with proposed membrane.

Membranes	Degradation Temperature / ° C	Ref.
SEBS[a]	430	[16]
PVT [b]	400	[17]
Si-sPS/A[c]	350	[22]
Na-PBI-ZP[d]	450	[44]
PVA–ZrP–Cs₂STA[e]	400	[49]
PAMPS-*co*-MMA[f]	400	[50]
Nafion®/SPEEK[g]	520	[51]
SGO-SPS-PE	480	This work

[a]*PolyStyrene-block-poly(Ethylene-ran-butylene)-Block-Polystyrene,* [b]*Poly(5-Vinyl Tetrazole),* [c]*Silicon-containing Sulfonated Polystyrene/Acrylate,* [d]*polybenzimidazole-Zirconium phosphate (ZP),* [e]*Polyvinyl alcohol and zirconium phosphate, cesium salt of heteropoly acid (PVA–ZrP–Cs2STA),* [f]*Copolymer methyl methacrylate and 2-acrylamido-2-methyl-1-propanesulfonic acid (PAMPS-co-MMA),* [g] *Sulfonated poly(ether ether ketone)s (SPEEKs).*

after 10 months and the results for degradation temperature were similar to the new membrane with a RSD% less than 3%. Also, the proposed membrane does not need any pre-treatment the same as Nafion membrane. Nafion membrane, before using in GDL must be pretreated in two steps (1) dipping in water 80 °C including H_2O_2 (5% m/m) and then (2) dipping H_2SO_4 solution. This pre-treatment takes 2-3h time. But the proposed membrane needs dipping in boiling water for 30 min and then in 1 M H_2SO_4 for 24 h.

CONCLUSION

GO was synthesized by modified Hummer's method and functionalized with SO_3-H. For sulfonated polystyrene used the method patented by *Makowski et al.* SPS composite membrane with SGO in PE was synthesized by a simple solvent cast method. Characterizations of the composites were carried out using FT-IR, SEM techniques. From the FT-IR studies on SGO-SPS-PE composites, the peak at 1141 cm⁻¹ is considered to be a measure of the degree of electron delocalization, 1493 and 1567 cm⁻¹ is C=C stretching of the benzenoid ring, The four sharp bands at 1009 cm⁻¹, 1039 cm⁻¹, 1128 cm⁻¹, 1179 cm⁻¹ show clearly SO_3 symmetric stretching. The SEM images of particles of SGO is shown clearly depict the diameter of particles are in the size range of about 100 nm -1 μm, and SEM image of the hybrid SGO-SPS-PE show that the hybrid SGO-SPS-PE a uniform matrix membrane had a dense structure. The TGA curves for composite membrane exhibit high thermal stability.

The results of dc conductivity show a strong dependence on the SGO in SPS-PE composites. Several PEM parameters, such as the water content, the proton conductivity of the membrane, the methanol permeability of the membrane, and the selectivity of the membrane, were tested. This membrane exhibit high IEC and water sorption compared to Nafion®117. Results show the synthesis composite membrane is very suitable for application in DMFC.

REFERENCES

[1] Ang Sh.M.C., Fraga E.S., Brandon N.P., Samsatli N.J., Brett D.J.L., Fuel Cell Systems Optimisation-Methods and Strategies, *Int. J. Hydrogen Energ.*, **36**:14678-14703 (2011).

[2] Yildirim M. H., Schwarz A., Stamatialis D.F., Wessling M., Impregnated Membranes for Direct Methanol Fuel Cells at High Methanol Concentrations, *J. Membrane Sci.*, **328**:127-133(2009).

[3] Hu Zh., Ogou T., Yoshinob M., Yamada O., Kita H., Okamoto K.I., Direct Methanol Fuel Cell Performance of Sulfonated Polyimide Membranes, *J. Power Sources,* **194**:674-682(2009).

[4] Xiang Y., Yang M., Guo Zh., Cui Zh., Alternatively Chitosan Sulfate Blending Membrane as Methanol-Blocking Polymer Electrolyte Membrane for Direct Methanol Fuel Cell, *J. Membrane Sci.,* **337**:318-323(2009).

[5] Nguyen T. H., Wang Ch., Wang X., Pore-Filling Membrane for Direct Methanol Fuel Cells Based on Sulfonated Poly(Styrene-Ran-Ethylene) and Porous Polyimide Matrix, *J. Membrane Sci.,* **342**: 208-214 (2009).

[6] Su Y.H., Liu Y.L., Wang D.M., Lai J.Y., Guiver M.D., Liu B., Increases in the Proton Conductivity and Selectivity of Proton Exchange Membranes for Direct Methanol Fuel Cells by Formation of Nanocomposites Having Proton Conducting Channels, *J. Power Sources*, **194**:206–213(2009).

[7] Kim J., Momma T., Osaka T., Cell Performance of Pd–Sn Catalyst in Passive Direct Methanol Alkaline Fuel Cell Using Anion Exchange Membrane, *J. Power Sources,* **189**:999-1002(2009).

[8] Cui Zh., Xing W., Liu Ch., Liao J., Zhang H., Chitosan/Heteropolyacid Composite Membranes for Direct Methanol Fuel Cell, *J. Power Sources,* **188**:24-29(2009).

[9] Wang J., Zhang H., Jiang Zh., Yang X., Xiao L., Tuning the Performance of Direct Methanol Fuel Cell Membranes by Embedding Multifunctional Inorganic Submicrospheres into Polymer Matrix, *J. Power Sources,* **188**:64-74(2009).

[10] Chen H., P. Pei, Song M., Lifetime Prediction And the Economic Lifetime of Proton Exchange Membrane Fuel Cells, *Appl. Energ.*, **142**:154-163(2015).

[11] Chouler J., Padgett G.A., Cameron P.J., Preuss K., Titirici M.M., Ieropoulos I., Lorenzo M.D., Towards Effective Small Scale Microbial Fuel Cells for Energy Generation from Urine, *Electrochim. Acta,* **192**:89–98(2016).

[12] Cho K.Y., Eom J.Y., Jung H.Y., Choi N.S., Lee Y. M., Park J.K., Choi J.H., Park K.W., Sung Y.E., Characteristics of PVdF Copolymer/Nafion Blend Membrane For Direct Methanol Fuel Cell (DMFC), *Electrochim. Acta,* **50**:583-588(2004).

[13] Dimitrova P., Friedrich K.A., Vogt B., Stimming U., Transport Properties of Ionomer Composite Membranes for Direct Methanol Fuel Cells, *J. Electroanal. Chem.*, **532**:75-83(2002).

[14] Mandanipour V., Noroozifar M.., Modarresi-Alam A.R, Khorasani-Motlagh M., Fabrication and Characterization of a Conductive Proton Exchange Membrane Based on Sulfonated Polystyrenedivinylbenzene Resin-Polyethylene (SPSDR-PE): Application in Direct Methanol Fuel Cells, *Iran. J. Chem. Chem. Eng.*, **36**:151-162(2017).

[15] Jung S., High-Performance Direct Methanol Fuel Cell with Optimized Membrane Electrode Assembly: a Theoretical Approach, *Int. J. Hydrogen Energ.,* 1-13(2016).

[16] Perrot C., Gonon L., Marestin C., Gebel G., Hydrolytic Degradation of Sulfonated Polyimide Membranes for Fuel Cells, *J. Membrane Sci.,* **379**: 207–214 (2011).

[17] Wang Y., Geder J., Schubert J.M., Dahl R., Pasel J., Peters R., Optimization of Adsorptive Desulfurization Process of Jet Fuels for Application in Fuel Cell Systems, *Fuel Process. Technol.*, **95**:144-153 (2012).

[18] Wei X., Yates M.Z., Nafion®/polystyrene-b-Poly(Ethylene-Ran-Butylene)-B-Polystyrene Composite Membranes with Electric Field-Aligned Domains for Improved Direct Methanol Fuel Cell Performance, *J. Power Sources,* **195**:736-743(2010).

[19] Li J., Wang J., Chen X., Lv Zh., Chen T., Wang T., A Highly Conductive Proton Exchange Membrane for High Temperature Fuel Cells Based on Poly(5-Vinyl Tetrazole) and Sulfonated Polystyrene, *Solid State Ionics,* **255**:128-134(2014).

[20] Xu J., Ma L., Han H., Ni H., Wang Z., Zhang H., Synthesis and Properties of a Novel Sulfonated Poly(Arylene Ether Ketone Sulfone) Membrane with a High β-Value for Direct Methanol Fuel Cell Applications, *Electrochim. Acta*, **146**:688-696 (2014).

[21] Kim D.J., Lee H.J., Nam S.Y., Sulfonated Poly(Arylene Ether Sulfone) Membranes Blended with Hydrophobic Polymers for Direct Methanol Fuel Cell Applications, *Int. J. Hydrogen Energ.*, **39**:17524-17532(2014).

[22] Zeng Q.H., Liu Q.L., Broadwell I., Zhu A.M., Xiong Y., Tu X.P., Anion Exchange Membranes Based on Quaternized Polystyrene-Block-Poly(Ethylene-ran-butylene)-Block-Polystyrene for Direct Methanol Alkaline Fuel Cells, *J. Membrane Sci.*, **349**: 237-243 (2010).

[23] Li Q., Jensen J.O., Savinell R.F., Bjerrum N.J., High Temperature Proton Exchange Membranes Based on Polybenzimidazoles for Fuel Cells, *Prog. Polym. Sci.*, **34**:449-477(2009).

[24] Zhong Sh., Cui X., Dou S., Liu W., Gao Y., Hong B., Improvement in Silicon-Containing Sulfonated Polystyrene/Acrylate Membranes by Blending and Crosslinking, *Electrochim. Acta*, **55**: 8410-8415 (2010).

[25] Abdrashitov E.F., Bokun V.Ch., Kritskaya D.A., Sanginov E.A., Ponomarev A.N., Dobrovolsky Y.A., Synthesis and Properties of the PVDF-Based Proton Exchange Membranes with Incorporated Cross-Linked Sulphonated Polystyrene for Fuel Cells, *Solid State Ionics*, **251**: 9-12 (2013).

[26] Li J., Cai W., Zhang Y., Chen Zh., Xu G., Cheng H., Novel Polyamide Proton Exchange Membranes with Bi-Functional Sulfonimide Bridges for Fuel Cell Applications, *Electrochim Acta*, **151**: 168-176 (2015).

[27] Yin Y., Wang J., Yang X., Du Q., Fang J., Jiao K., Modeling of High Temperature Proton Exchange Membrane Fuel Cells with Novel Sulfonated Polybenzimidazole Membranes, *J. Electrochem. En. Conv. Stor.*, **39**:13671-13680 (2014).

[28] Jiang Zh., Zhao X., Manthiram A., Arumugam Manthiram, Sulfonated poly(ether ether ketone) Membranes with Sulfonated Graphene Oxide Fillers for Direct Methanol Fuel Cells, *Int. J. Hydrogen Energ.*, **38**:5875-5884 (2013).

[29] Chien H.Ch., Tsai L.D., Huang Ch.P., Kang Ch.Y., Lin J.N., Chang F.Ch., Sulfonated Graphene Oxide/Nafion Composite Membranes for High-Performance Direct Methanol Fuel Cells, *Int. J. Hydrogen Energ.*, **38**:13792-13801(2013).

[30] Lin C.W., Lu Y.S., Highly Ordered Graphene Oxide Paper Laminated with a Nafion Membrane for Direct Methanol Fuel Cells, *J. Power Sources*, **237**: 187-194(2013).

[31] Wang L.Sh., Lai A.N., Lin Ch.X., Zhang Q.G., Zhu A.M., Liu Q.L., Orderly Sandwich-Shaped Graphene Oxide/Nafion Composite Membranes for Direct Methanol Fuel Cells, *J. Membrane Sci.*, **492**:58-66 (2015).

[32] Cao Y.C., Xu C., Wu X., Wang X., Xing L., Scott K.A., A Poly (ethylene oxide)/Graphene Oxide Electrolyte Membrane for Low Temperature Polymer Fuel Cells, *J. Power Sources*, **196**:8377-8363(2011).

[33] Lian Y.F., Liu Y.X., Jiang T., Shu J., Lian H.Q., Cao M.H., Enhanced Electromechanical Performance of Graphite Oxide-Nafion Nanocomposite Actuator, *J. Phys. Chem. C.*, **114**: 9659-9663 (2010).

[34] Yang X.M., Li L.A., Shang S.M., Tao X.M., Synthesis and Characterization of Layer-Aligned Poly(Vinyl Alcohol)/ Graphene Nanocomposites, *Polymer,* **51**:3431-3435(2010).

[35] Scott R. and K., Freestanding Sulfonated Graphene Oxide Paper: A New Polymer Electrolyte for Polymer Electrolyte Fuel Cells, *Chem. Commun.*, **48**:5584-5586(2012).

[36] Gahlot S., Sharma P.P., Kulshrestha V., Jha P.K., SGO/SPES-Based Highly Conducting Polymer Electrolyte Membranes for Fuel Cell Application, *ACS Appl. Mater. Inter.,* **6**:5595(2014).

[37] Jiang Z., Zhao X., Fu Y., Manthiram A., Composite Membranes Based on Sulfonated Poly(Ether Ether Ketone) and SDBS-Adsorbed Graphene Oxide for Direct Methanol Fuel Cells, *J. Mater. Chem.*, **22**:24862(2012).

[38] Zarrin H., Higgins D., Jun Y., Chen Z., Fowler M., Functionalized Graphene Oxide Nanocomposite Membrane for Low Humidity and High Temperature Proton Exchange Membrane Fuel Cells, *J. Phys. Chem. C.*, **115**: 20774 (2011).

[39] Makowski H.S., Lundberg R.D., Singhal G.H., *US Ppaent 870:841-*(1975).

[40] Martins R.C., Ruggeri G., De Paoli M-A., Synthesis in Pilot Plant Scale and Physical Properties of Sulfonated Polystyrene, *J. Braz Chem. Soc.,* **14**: 797-802 (2003).

[41] Hummers W.S., Offeman R.E., Preparation of Graphitic Oxide, *J. Am. Chem. Soc.*, 80:1339(1958).

[42] Mandanipour V., Noroozifar M., Modarresi-Alam A.R., Preparation of Modified Sulfonated Poly(Styrene Divinylbenzene) with Polyaniline as a New Polymer Electrolyte Membrane for Direct Methanol Fuel Cell, *Int. J. Electrochem. Sci.*, **11**:5302-5317(2016).

[43] Enotiadis A., Angjeli K., Baldino N., Nicotera I., Gournis D., Graphene-Based Nafion Nanocomposite Membranes: Enhanced Proton Transport and Water Retention by Novel Organo-Functionalized Graphene Oxide Nanosheets, *Small*, **8**:3338(2012).

[44] Shukla A., Dhanasekaran P., Sasikala S., Nagaraju N., Bhat S.D., Pillai V.K., Covalent Grafting of Polystyrene Sulfonic Acid on Graphene Oxide Nanoplatelets to form a Composite Membrane Electrolyte with Sulfonated Poly(Ether Ether Ketone) for Direct Methanol Fuel Cells, *J. Membrane Sci.*, **595**:117484(2020).

[45] Ahmad H., Kamarudin S.K., Hasran U.A., Daud W.R.W., A Novel Hybrid Nafion-PBI-ZP Membrane for Direct Methanol Fuel Cells, *Int. J. Hydrogen Energ.*, **36**:14668-14677 (2011).

[46] Tai C.C., Chen C.L., Liu C.W., Computer Simulation to Investigate Proton Transport and Conductivity in Perfluorosulfonate Ionomeric Membrane, *Int. J. Hydrogen Energ.*, **42**: 3981-3986 (2017).

[47] Morris D.R., Sun X., Water-Sorption and Transport Properties of Nafion 117, *J. Appl. Polym. Sci.*, **50**:1445-1452(1993).

[48] Li Y., Hoorfar M., Shen K., Fang J., Yue X., Jiang Zh., Development of a Crosslinked Pore-filling Membrane with an Extremely Low Swelling Ratio and Methanol Crossover for Direct Methanol Fuel Cells, *Electrochim Acta*, **232:**226-235(2017).

[49] Chen Ch-Y., Garnica-Rodriguez J.I., Duke M.C., Dalla Costa R.F., Dicks A.L., da Costa J.C.D., Nafion/polyaniline/Silica Composite Membranes for Direct Methanol Fuel Cell Application, *J. Power Sources*, **166**:324-(2007).

[50] Arbizzani C., Donnadio A., Pica M., Sganappa M., Varzi A., Casciola M., Mastragostino M., Methanol Permeability and Performance of Nafion–Zirconium Phosphate Composite Membranes in Active and Passive Direct Methanol Fuel Cells, *J. Power Sources*, **195**:7751-7756(2010).

[51] Helen M., Viswanathan B., Srinivasa Murthy S., Fabrication and Properties of Hybrid Membranes Based on Salts of Heteropolyacid, Zirconium Phosphate and Polyvinyl Alcohol, *J. Power Sources*, **163**:433-439(2006).